
Policy Gradients Incorporating the Future

David Venuto^{1,2}, Elaine Lau², Doina Precup^{1,2,3}, Ofir Nachum⁴

¹Mila, ²McGill University, ³DeepMind, ⁴Google Brain
 {david.venuto, tsoi.lau}@mail.mcgill.ca
 dprecup@cs.mcgill.ca, ofirnachum@google.com

Abstract

Reasoning about the future – understanding how decisions in the present time affect outcomes in the future – is one of the central challenges for reinforcement learning (RL), especially in highly-stochastic or partially observable environments. While predicting the future directly is hard, in this work we introduce a method that allows an agent to “look into the future” without explicitly predicting it. Namely, we propose to allow an agent, during its training on past experience, to observe what *actually* happened in the future at that time, while enforcing an information bottleneck to avoid the agent overly relying on this privileged information. This gives our agent the opportunity to utilize rich and useful information about the future trajectory dynamics in addition to the present. Our method, Policy Gradients Incorporating the Future (PGIF), is easy to implement and versatile, being applicable to virtually any policy gradient algorithm. We apply our proposed method to a number of off-the-shelf RL algorithms and show that PGIF is able to achieve higher reward faster in a variety of online and offline RL domains, as well as sparse-reward and partially observable environments.

1 Introduction

Fundamentally, reinforcement learning (RL) is composed of gathering useful information (*exploration*) and assigning credit to that information (*credit assignment*). Both of these problems present their own unique learning challenges. In this work, we focus on credit assignment, which refers to the challenge of matching observed outcomes in the future to decisions made in the past. Humans appear to do this in a sample efficient manner [16], and so it is natural to expect our own RL agents to do so as well.

One of the most popular approaches to credit assignment, known as *model-free* RL, is to learn a value function to approximate the future return given a starting state and action. The value function is learned using experience of the agent acting in the environment via temporal difference (TD) methods [37], which regress the value function to a target based on a combination of groundtruth returns achieved in the environment and the approximate value function itself. The need to *bootstrap* learning of the value function on its own estimates is known to lead to difficulties in practice, where one must achieve a careful balance between bias and variance [14, 47, 33, 22]. If a slight imbalance arises, the consequences can be disastrous for learning [43, 44, 39]. For example, in offline RL this issue is so pronounced that algorithms must apply strong regularizations on both learned policy and value function to achieve stable performance [48, 19, 51, 23].

The model-free approach plays dual to the *model-based* approach, where an agent learns a dynamics and reward model of the environment, and then learns an agent to optimize behavior in this model. Thus, credit assignment boils down to utilizing an appropriate planning algorithm that can perform multiple rollouts in the model, effectively allowing the agent to “look into the future” [31, 28] to determine cause-and-effect [38, 30, 2]. While model-based RL may appear more straightforward, learning an accurate model is a challenge in practice, presenting its own sample-efficiency problems

[46] as well as memory and computational issues [52]. Model-based approaches are thus most beneficial when the environment exhibits some level of regularity [1].

Beyond these issues, credit assignment in both model-free and model-based RL is further exacerbated by *partially observable* environments, in which the full environment state is not known to the learning agent. Thus it is infeasible to predict future events accurately. When applied to such non-Markovian domains, model-free algorithms relying on bootstrapping and value function approximation tend to be biased [35]. On the other hand for model-based approaches, learning an accurate dynamics model in such domains is a difficult, potentially ill-defined problem [36, 6].

In this work, we aim to circumvent these challenges. We propose a simple modification to model-free RL that allows the learned policy and value function to “look into the future” but without the need to learn an accurate model. Namely, we propose to modify the policy and value function to not only condition on the presently observed state and action but also on the subsequent trajectory (sampled by the agent as it was interacting with the environment) following this state and action. This way, our method mitigates potential approximation or feasibility issues in accurately modeling the future. To ensure that the learned policy and value function remains relevant during inference (i.e., data collection) when the future trajectory is unavailable, we place an *information bottleneck* [32, 41] on the additional inputs, encouraging the learned functions to minimize their reliance on this privileged information. One may thus view our method as an instance of *teacher forcing* or *Z-forcing* [11, 20] where our student is the learned policy and value function and the teacher is some function of the information in the future trajectory.

Practically, our method, Policy Gradients Incorporating the Future (PGIF), is easy to implement. We use either a backwards RNN or a transformer to inject downstream information from the observed trajectories by way of latent variables, with a KL divergence regularization on these latents. We apply PGIF on top of a variety of off-the-shelf RL algorithms, including RNN-based PPO [34], SAC [13], and BRAC [48], and evaluate these algorithms on online and offline RL as well as sparse-reward and partially observable environments. In all of these domains, we demonstrate the ability of PGIF to achieve higher returns faster compared to these existing RL algorithms on their own, thus showing that our proposed method is both versatile and beneficial in practice.

2 Background and Notation

We begin by providing a brief overview of the notation and preliminary concepts that we will use in our later derivations.

Markov Decision Processes (MDPs) MDPs are defined by a tuple $\langle \mathcal{S}, \mathcal{A}, \mathbb{P}, R, \rho_0, \gamma \rangle$ where \mathcal{S} is a set of *states*, \mathcal{A} is a set of *actions*, \mathbb{P} is a transition kernel giving a probability $\mathbb{P}(s'|s, a)$ over next states given the current state and action, $R : \mathcal{S} \times \mathcal{A} \rightarrow [R_{\min}, R_{\max}]$ is a reward function, ρ_0 is an initial state distribution, and $\gamma \in [0, 1)$ is a discount factor. An agent in this MDP is a stationary policy π giving a probability $\pi(a|s)$ over actions at any state $s \in \mathcal{S}$. A policy π interacts with the MDP by starting at $s_0 \sim \rho_0$ and then at time $t \geq 0$ sampling an action $a_t \sim \pi(s_t)$ at which point the MDP provides an immediate reward $R(s_t, a_t)$ and transitions to a next state $s_{t+1} \sim \mathbb{P}(s_t, a_t)$. The interaction ends when the agent encounters some terminal state s_T .

The value function $V^\pi : \mathcal{S} \rightarrow \mathbb{R}$ of a policy is defined as $V^\pi(s) = \mathbb{E}_\pi[\sum_{t=0}^{T-1} \gamma^t r_t | s_0 = s]$, where \mathbb{E}_π denotes the expectation of following π in the MDP and T is a random variable denoting when a terminal state is reached. Similarly, the state-action value function $Q^\pi : \mathcal{S} \times \mathcal{A} \rightarrow \mathbb{R}$ is defined as $Q^\pi(s, a) = \mathbb{E}_\pi[\sum_{t=0}^{T-1} \gamma^t r_t | s_0 = s, a_0 = a]$. The advantage A^π is then given by $A^\pi(s, a) = Q^\pi(s, a) - V^\pi(s)$. We denote ρ_π as the distribution over trajectories $\tau = (s_0, a_0, r_0, \dots, s_T)$ sampled by π when interacting with the MDP.

During learning, π is typically parameterized (e.g., by a neural network), and in this case, we use π_θ to denote this parameterized policy with learning parameters given by θ . The policy gradient theorem [40] states that, in order to optimize the RL objective $\mathbb{E}_{s_0 \sim \rho_0}[V^\pi(s_0)]$, a parameterized policy should be updated with respect to the loss function,

$$J_{\text{PG}}(\pi_\theta) = \mathbb{E}_{\tau \sim \rho_{\pi_\theta}} \left[\sum_{t=0}^{T-1} \gamma^t \cdot \hat{Q}_t \log \pi_\theta(a_t | s_t) \right], \quad (1)$$

where \hat{Q}_t is an unbiased estimate of $Q^\pi(s_t, a_t)$. In the simplest case, \hat{Q}_t is the empirically observed future discounted return following s_t, a_t . In other cases, an approximate Q -value or advantage function is incorporated to trade-off between the bias and variance in the policy gradients. When the Q or V value function is parameterized, we will use ψ to denote its parameters. For example, the policy gradient loss with a parameterized Q_ψ is given by,

$$J_{\text{PG}}(\pi_\theta, Q_\psi) = \mathbb{E}_{\tau \sim \rho_{\pi_\theta}} \left[\sum_{t=0}^{T-1} \gamma^t \cdot Q_\psi(s_t, a_t) \log \pi_\theta(a_t | s_t) \right]. \quad (2)$$

The value function Q_ψ is typically learned via some regression-based temporal differencing method. For example,

$$J_{\text{TD}}(Q_\psi) = \mathbb{E}_{\tau \sim \rho_{\pi_\theta}} \left[\sum_{t=0}^{T-1} (\hat{Q}_t - Q_\psi(s_t, a_t))^2 \right]. \quad (3)$$

Stochastic Latent Variable Models In our derivations, we will utilize parameterized policies and value functions conditioned on auxiliary inputs given by stochastic latent variables. That is, we consider a latent space \mathcal{Z} , typically a real-valued vector space. We define a parameterized policy that is conditioned on this latent variable as $\pi_\theta(a|s, z)$ for $a \in \mathcal{A}, s \in \mathcal{S}, z \in \mathcal{Z}$; i.e., π_θ takes in states and latent variables and produces a distribution over actions. In this way, one can consider the latent variable z as modulating the behavior of π_θ in the MDP. During interactions with the MDP or during training, the latent variables themselves are generated by some stochastic process, thus determining the behavior of π_θ . For example, in the simplest case z may be sampled from a latent prior $p_{v(z)}(z|s)$, parameterized by $v^{(Z)}$. Thus, during interactions with the MDP actions a_t are sampled as $a_t \sim \pi_\theta(s_t, z_t), z_t \sim p_{v(z)}(s_t)$.

We treat parameterized latent variable value functions analogously. Specifically, we consider a latent space \mathcal{U} and a parameterized Q -value function as $Q_\psi(s, a, u)$. A prior distribution over these latent variables may be denoted by $p_{v(u)}(u|s)$.

3 Policy Gradients Incorporating the Future

Our method aims to allow a policy during training to leverage *future* information for learning control. We propose to utilize stochastic latent variable models to this end. Namely, we propose to train π_θ and Q_ψ with latent variables $(\mathbf{z}, \mathbf{u}) = \{(z_t, u_t)\}_{t=0}^{T-1}$ sampled from a learned function $q_\phi(\tau)$ which has access to the full trajectory. For example, the PGIF form of the policy gradient objective in (2) may be expressed as

$$J_{\text{PGIF, PG}}(\pi_\theta, Q_\psi, q_\phi) = \mathbb{E}_{\tau \sim \rho_{\pi_\theta}, (\mathbf{z}, \mathbf{u}) \sim q_\phi(\tau)} \left[\sum_{t=0}^{T-1} \gamma^t \cdot Q_\psi(s_t, a_t, u_t) \log \pi_\theta(a_t | s_t, z_t) \right]. \quad (4)$$

The PGIF form of the temporal difference objective in (3) may be expressed analogously as,

$$J_{\text{PGIF, TD}}(Q_\psi, q_\phi) = \mathbb{E}_{\tau \sim \rho_{\pi_\theta}, \mathbf{u} \sim q_\phi(\tau)} \left[\sum_{t=0}^{T-1} (\hat{Q}_t - Q_\psi(s_t, a_t, u_t))^2 \right]. \quad (5)$$

It is clear that any RL objective which trains policies and/or value functions on trajectories can be adapted to a PGIF form in a straightforward manner. For example, in our experiments we will apply PGIF to an LSTM-based PPO [34], SAC [13], and BRAC [48].

While the PGIF-style objectives above adequately achieve our aim of allowing a policy to leverage future trajectory information during training, they also present a challenge during inference. When performing online interactions with the environment, one cannot evaluate $q_\phi(\tau)$, since the full trajectory τ is not yet observed.

Therefore, while we want to give π_θ and Q_ψ the ability to look at the full τ during training, we do not want their predictions to overly rely on this privileged information. To this end, we introduce a regularization on q_ϕ in terms of a KL divergence from a prior distribution $p_v(\tau) := \{p_v(z_t, u_t | s_t)\}_{t=0}^{T-1}$ which conditions (z_t, u_t) only on s_t . Thus, in the case of policy gradient, the full loss is,

$$J_{\text{PGIF-KL}}(\pi_\theta, Q_\psi, q_\phi) = J_{\text{PGIF, PG}}(\pi_\theta, Q_\psi, q_\phi) + \beta \mathbb{E}_{\tau \sim \rho_{\pi_\theta}} [D_{\text{KL}}(q_\phi(\tau) \| p_v(\tau))], \quad (6)$$

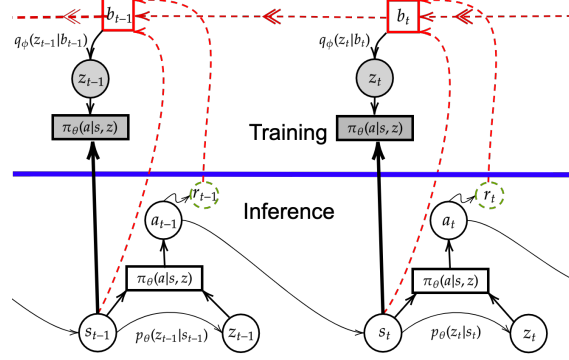


Figure 1: The architecture of the model. Our inference model $q_\phi(z)$ uses a backwards hidden state b_t to approximate dependencies of z_t on the future of the trajectory. The blue line separates the data collection and policy gradient training steps in our algorithm and the red lines represent information flowing into the backwards RNN. Grey variables are used during training and white variables are used during data collection. **Top:** we show the training model where the policy gradient loss is calculated with backwards RNN hidden state information. **Bottom:** we show the data collection phase of the algorithm utilizing latent variables sampled from the latent prior.

where β is the weight of the divergence term. The introduction of this prior thus solves two problems: (1) it encourages the learned policies and value functions to not overly rely on information beyond the immediate state; (2) it provides a mechanism for inference, namely using latent samples from $p_v(s)$ when interacting with the environment.

Parameterization of q_ϕ In our implementation, we parameterize $q_\phi(\tau)$ as an RNN operating in reverse order on τ . Specifically, we use an LSTM network to process the states in τ backwards, to yield LSTM hidden states $\mathbf{b} = \{b_t\}_{t=0}^{T-1}$. The function q_ϕ is then given by Gaussian distributions with mean and variance at time t derived from the backwards state b_t . In practice, to avoid potential interfering gradients from the objectives of π_θ and Q_ψ , we use separate RNNs with independent parameters $q_\phi(z)$, $q_\phi(u)$ for z_t , u_t , respectively. See Figure 1 for a graphical diagram of the training and inference procedure for PGIF. In our empirical studies below, we will also show that a transformer [45] can be used in place of an RNN, providing more computational efficiency and potentially allowing for better propagation of information over time.

3.1 Variational Information Bottleneck Interpretation

The KL regularization we employ above may be interpreted as a variational information bottleneck, constraining the mutual information between the latent variable distribution and the trajectory τ . Here we provide a brief derivation establishing this equivalence.

For simplicity, we consider a specific timestep $t \in \mathbb{N}$ and a starting state $s_t = s$. Let $\mathcal{T}_{\geq t}$ denote the random variable for all information contained after and including timestep t in trajectory τ induced by π . Let \mathcal{U}_t be the random variable for latents u_t induced by $q_\phi(\tau_{\geq t})$ conditioned on all steps in the trajectory after and including t . Consider a constrained objective minimizing $J_{\text{PGIF,TD}}$ while enforcing an upper bound I_{\max} on the mutual information between the distribution of trajectory steps and the distribution of latent variables $I(\mathcal{T}_{\geq t}, \mathcal{U}_t | s_t = s)$. This objective is given by,

$$\begin{aligned} \min_{\psi, \phi} \quad & J_{\text{PGIF,TD}}(Q_\psi, q_\phi | s_t = s) := \mathbb{E}_{\tau \sim \rho_{\pi_\theta}(\cdot | s_t = s), u_t \sim q_\phi(\tau_{\geq t})} [(\hat{Q}_t - Q_\psi(s_t, a_t, u_t))^2] \\ \text{s.t.} \quad & I(\mathcal{T}_{\geq t}, \mathcal{U}_t | s_t = s) \leq I_{\max}. \end{aligned} \quad (7)$$

Recall the definition of mutual information:

$$\begin{aligned} I(\mathcal{T}_{\geq t}, \mathcal{U}_t | s_t = s) &= \int p(\tau_{\geq t}, u_t | s_t = s) \log \frac{p(\tau_{\geq t}, u_t | s_t = s)}{p(\tau_{\geq t} | s_t = s)p(u_t | s_t = s)} du_t d\tau_{\geq t} \\ &= \int \rho_{\pi_\theta}(\tau_{\geq t} | s_t = s) q_\phi(u_t | \tau_{\geq t}) \log \frac{q_\phi(u_t | \tau_{\geq t})}{p(u_t | s_t = s)} du_t d\tau_{\geq t}, \end{aligned} \quad (8)$$

where $p(u_t|s_t = s)$ is the marginal distribution over the latent variable $p(u_t|s_t = s) = \int q_\phi(u_t|\tau_{\geq t})\rho_\pi(\tau_{\geq t}|s_t = s)d\tau_{\geq t}$. This marginal is intractable to compute directly, and so to approximate this marginal we introduce a variational distribution $h(u_t|s_t = s)$. By definition we know that $D_{\text{KL}}[p(u_t|s_t = s)||h(u_t|s_t = s)] \geq 0$. We can then see that $\int p(u_t|s_t = s) \log p(u_t|s_t = s) du_t \geq \int p(u_t|s_t = s) \log h(u_t|s_t = s) du_t$. We therefore derive the upper bound for use in (7) as,

$$\begin{aligned} I(\mathcal{T}_{\geq t}, \mathcal{U}_t|s_t = s) &\leq \int \rho_\pi(\tau_{\geq t}|s_t = s) q_\phi(u_t|\tau_{\geq t}) \log \frac{q_\phi(u_t|\tau_{\geq t})}{h(u_t|s_t = s)} du_t d\tau_{\geq t} \\ &\leq \mathbb{E}_{\tau \sim \rho_{\pi_\theta}(\cdot|s_t=s)} \left[D_{\text{KL}}(q_\phi(u|\tau_{\geq t})||h(u_t|s_t = s)) \right]. \end{aligned} \quad (9)$$

We can subsume the constraint into the objective as,

$$\min_{\psi, \phi} J_{\text{PGIF,TD}}(Q_\psi, q_\phi|s_t = s) + \beta \left(\mathbb{E}_{\tau \sim \rho_{\pi_\theta}(\cdot|s_t=s)} [D_{\text{KL}}(q_\phi(\tau_{\geq t})||h(u_t|s_t = s))] - I_{\text{max}} \right).$$

By taking h to be our learned prior p_v , we achieve the single step ($s_t = s$), TD analogue of the PGIF objective in (6), offset by a constant $\beta \cdot I_{\text{max}}$.

3.2 Z-Forcing with Auxiliary Losses

While our proposed training architecture enables the policy and value function to look at the full trajectory τ , in practice it may be difficult for the trajectory information to propagate, especially in settings with highly stochastic learning signals. In fact, it is known that such latent variable models may ignore the latent variables due to optimization issues, completely negating any potential benefit [4]. To circumvent these issues, we make use of the idea of *Z-forcing* [12], which employs auxiliary losses and models to force the latent variables to encode information about the future. We denote this loss as $J_{\text{Ax}}(\zeta)$ where ζ is the set of parameters in any auxiliary models, and elaborate on the main forms of this loss which we consider below.

State based forcing (Force) A simple way to force state information to be encoded is to derive conditional generative models $p_\zeta(b_t|z_t)$ over the backwards states given the inferred latent variables $z_t \sim q_{\phi(z)}(z_t|b_t)$, and similarly for the latents u_t . We can write this auxiliary objective as a maximum log-likelihood loss $J_{\text{Ax}}(\zeta) = -\mathbb{E}_{q_{\phi(z)}(z_t|b_t)} [\log p_\zeta(b_t|z_t)]$. This way, we enforce the noisy mapping $b_t \rightarrow z_t$ defined by $q_{\phi(z)}$ to not be *too noisy* so as to completely remove any information from b_t .

Value prediction networks (VPN) A more sophisticated approach to force information to be propagated is to use an autoencoder-like, model-based auxiliary loss. To this end, we take inspiration from VPNs [25], and apply an auxiliary loss that uses b_t to predict future rewards, values, and discounts. Note that, in principle, b_t already has access to this information, by virtue of the backwards RNN or transformer conditioned on the future trajectory. Thus, this auxiliary loss only serves to enforce that the RNN or transformer dutifully propagates this information from its inputs. We also note that, in contrast to the state based forcing described above, this approach only enforces b_t to contain the relevant information, and it is up to the RL loss whether this information should be propagated to the latents z_t, u_t .

In more detail, the VPN loss introduces the following additional learnable functions:

- a) Encoding network : $f^{(\text{enc})} : s \rightarrow x$
- b) Outcome encoder: $f^{(\text{out})} : x, a \rightarrow \hat{\gamma}, \hat{r}$
- c) Value predictor: $f^{(\text{val})} : x \rightarrow \hat{V}(x)$
- d) Transition predictor: $f^{(\text{trans})} : x, a \rightarrow \hat{x}'$

Given a backwards state b_t , we first embed this to $x_t^0 = f^{\text{emb}}(b_t)$ with (a). We then make predictions on future rewards \hat{r}_t^l , transition dynamics \hat{x}_t^l , discounts $\hat{\gamma}_t^l$, and values $\hat{V}(x_t^l)$ using (b, c, d) for $l = 0, \dots, k$. Finally, we compute the VPN loss as,

$$J_{\text{VPN}}^t = \sum_{l=0}^{k-1} (R_{t+l} - \hat{V}(x_t^l))^2 + (r_{t+l} - \hat{r}_t^l)^2 + (\log_\gamma \gamma_{t+l} - \log_\gamma \hat{\gamma}_t^l)^2, \quad (10)$$

where R_{t+l} is the empirically observed future discounted reward in the trajectory. The full auxiliary loss $J_{\text{Ax}}(\zeta)$ is then given by summing up the loss in (10) over all timesteps in all trajectories.

3.3 Full Algorithm

The full learning objective for PGIF is thus composed of three components: First, a latent-variable augmented RL objective, e.g., policy gradient as shown in (4). Second, a KL regularizer, e.g., as shown in (6). Finally, an auxiliary loss, given by either state based forcing (Force) or value prediction networks (VPN). We present an example pseudocode of a PGIF-style policy gradient with learned value function in Algorithm 1.

See the Appendix for further details, including how to adaptively tune the coefficients on the KL and auxiliary loss components as well as more specific pseudocode algorithms for advantage policy gradient and soft actor-critic.

Algorithm 1 PGIF Algorithm with State-Action Value Function Estimation

Require: Initial parameters: $\theta, v^{(U)}, v^{(Z)}, \phi^{(U)}, \phi^{(Z)}, \psi, \zeta_{PG}, \zeta_{TD}$, **Weights:** $\alpha_{PG}, \alpha_{TD}, \beta_{PG}, \beta_{TD}$

- 1: **for** policy-step $k = 0, 1, 2, \dots, N$ **do**
- 2: Collect set of Trajectories $\mathcal{D} = \{\tau_i, \dots\}$:
- 3: **repeat**
- 4: $z_t \sim p_{v^{(Z)}}(z_t)$
- 5: Execute: $\pi_\theta(a_t|s_t, z_t)$ and observe r_t, s_{t+1} from environment.
- 6: **until** episode termination
- 7: **for** Trajectory: $\tau_i \in \mathcal{D}$ **do**
- 8: $\mathbf{b}^Z = \text{BackwardsLSTM}^Z(\tau_i)$ (Operates over the entire trajectory)
- 9: $\mathbf{b}^U = \text{BackwardsLSTM}^U(\tau_i)$
- 10: $\tau_i = \tau_i \cup \{\mathbf{b}^Z, \mathbf{b}^U\}$
- 11: $\forall \{\mathbf{s}, \mathbf{a}, \mathbf{r}, \mathbf{b}^Z, \mathbf{b}^U\} \in \mathcal{D}$:
- 12: Derive $J_{\text{Ax-PG}}(\zeta_{PG}), J_{\text{Ax-TD}}(\zeta_{TD})$ according to any auxiliary loss.
- 13: $D_{\text{TD}} = D_{\text{KL}}(q_{\phi^{(U)}}(\mathbf{u}|\mathbf{b}^U) \| p_{v^{(U)}}(\mathbf{u}|\mathbf{s}))$
- 14: $J_{\text{TD}} = \mathbb{E}_{\tau \in \mathcal{D}} [J_{\text{PGIF,TD}}(Q_\psi, q_{\phi^{(U)}}) + \alpha_{\text{TD}} J_{\text{Ax-TD}}(\zeta_{TD}) + \beta_{\text{TD}} D_{\text{TD}}]$
- 15: $D_{\text{PG}} = D_{\text{KL}}(q_{\phi^{(Z)}}(\mathbf{z}|\mathbf{b}^Z) \| p_{v^{(Z)}}(\mathbf{z}|\mathbf{s}))$
- 16: $J_{\text{PG}} = \mathbb{E}_{\tau \in \mathcal{D}} [J_{\text{PGIF,PG}}(\pi_\theta, Q_\psi, q_{\phi^{(Z)}}) + \alpha_{\text{PG}} J_{\text{Ax-PG}}(\zeta_{PG}) + \beta_{\text{PG}} D_{\text{PG}}]$
- 17: Update all parameters w.r.t: J_{PG} and J_{TD}

4 Related Work

We review relevant works in the literature in this section.

Incorporating the future Recent works in model-based RL have considered incorporating the future by way of dynamically leveraging rollouts of various horizon lengths and then using them for policy improvement [5]. Z-forcing and stochastic dynamics models have been applied directly to learning environmental models and for behavioral cloning while incorporating the future but not for online or offline continuous control [18]. Our present work is unique for incorporating Z-forcing and conditioning on the future in the model-free RL setting.

Hindsight Hindsight credit assignment introduces the notion of incorporating the future of a trajectory by assigning credit based on the likelihood of an action leading to an outcome in the future [14]. These methods were extended using a framework similar to ours, leveraging a backwards RNN to incorporate information in hindsight [21]. Still, there are a number of differences compared to our own work. First, in these previous works only the value function (rather than both the value and policy functions) is provided access to the future trajectory. Second, there is no KL information bottleneck; rather information is constrained via an action prediction objective. Third, these previous works do not employ any Z-forcing, while it is well-known that learning useful latent variables in the presence of an autoregressive decoder is difficult without Z-forcing [3]; in fact, in our own preliminary experiments we found our algorithm performs significantly worse without any auxiliary losses. Finally, our method is more versatile, being applicable to off-policy and offline RL settings rather than purely on-policy RL, as in these previous works. Nevertheless, it is an interesting avenue for future work to investigate how to combine the best of both approaches, especially with respect to

guarantees on variance reduction of policy gradient estimators [24] and hierarchical policy learning [49].

Combining model-based and model-free RL Our proposed PGIF is a way of enabling a model-free RL algorithm to “look into the future”. Although we do not learn explicit models of the MDP, our work may nevertheless be considered as combining elements of both model-based and model-free RL. Previous works have also claimed to do this, although in distinct ways. For example, previous work has proposed learning a low dimensional encoding of the environment and then performing planning in this abstract representation along with model-free RL [1]. VPNs [25] improve representations in model-based RL, and use a single network along with supervised learning to learn transition and reward dynamics in an abstract representation of the state space. Attention augment agents utilize dynamics model roll-outs as input during policy optimization [31]. Our work takes a very different approach and incorporates a representation of future information using the hidden states of a backwards RNN, while leveraging VPN-style losses only to enforce information in the RNN to be propagated from inputs to outputs.

Learning stochastic latent variable RNNs Deriving an approximate posterior over stochastic latent variables [3] conditioned on a backwards RNN hidden state has been practically useful in RNNs [12] and has been able to overcome being trapped in local minima [17]. Z-forcing [12] is able to learn useful latent variables that capture higher level representations even with a strong auto-regressive decoder, by reconstructing hidden states in a backwards RNN. We use the main methods from Z-forcing to force our variables to learn a useful representation of the trajectory for the agent. Our method employs an auxiliary signal similar to [17] to design a cost with good convergence properties. Our work is a novel application of these stochastic latent variable RNNs in online and offline policy gradient methods.

Auxiliary objectives in RL Incorporating auxiliary objectives in RL generally takes the form of intrinsic rewards. State-space density models have been used to derive intrinsic rewards that incentivize exploration, challenging the agent to find states that generate “surprise” [27]. Other works use the prediction error in an inverse model as a metric for curiosity [29]. The auxiliary objectives we utilize in this work serve the purpose of improving the incorporation of future dynamics information into policy optimization.

5 Experiments

We now provide a wide array of empirical evaluations of our method, PGIF, encompassing tasks with delayed rewards, sparse rewards, online access to the environment, offline access to the environment, and partial observability.

In our online RL experiments, we compare against Soft Actor Critic (SAC) [13] and Proximal Policy Optimization (PPO) [34] with an LSTM layer in the policy network. The comparison with PPO is particularly important since this method also leverages a form of artificial memory of the past (but not forward-looking like in PGIF). SAC is a state-of-the-art model-free RL method that employs a policy entropy term in a policy gradient objective and shows optimal performance and stability when compared with other online deep RL benchmarks. We show the hyper-parameters for each experiment in the Appendix. In addition, we explore using our method with a transformer as opposed to an LSTM as the backwards networks.

5.1 Credit Assignment

We first aim to show that our method is highly effective in an environment where credit assignment is the paramount objective. We examine the Umbrella-Length task from BSUITE [26], a task involving a long sequential episode where only the first observation (a forecast of rain or shine) and action (whether to take an umbrella) matter, while the rest of the sequence contains random unrelated information. A reward of +1 is given at the end of the episode if the agent chooses correctly to take the umbrella or not depending on the forecast. This difficult task is used to test the agent’s ability to assign credit correctly to the first decision. We evaluate PGIF-versions of SAC and PPO to vanilla SAC [13] as well as a PPO-LSTM [34] baseline. Results are presented in Table 1. We see that our method is able to achieve best performance, improving on the baselines by at least 50%.

This suggests that the PGIF agent is able to effeciciently and accurately propogate information about the final reward to the initial timestep, more so than either the one-step backups used in SAC or the multi-step return regressions used in PPO-LSTM can.

Method	Mean Bsuite-score
PPO-LSTM	0.33 ± 0.09
SAC	0.41 ± 0.03
PGIF-PPO (VPN)	0.46 ± 0.09
PGIF-PPO (Force)	0.26 ± 0.10
PGIF-SAC (VPN)	0.60 ± 0.04
PGIF-SAC (Force)	0.58 ± 0.08

Table 1: Performance on the Umbrella-Length environment. We run our model for 1000 episodes steps over 5 random seeds. The BSuite score is calculated in terms of the regret normalized [random, optimal] \rightarrow [0, 1] (higher is better). The number after \pm is the standard deviation.

5.2 Sparse Rewards

To test the performance of our method in a sparse reward setting, we utilize the AntMaze environment [7] where we have a simple U-shaped maze with a goal at the end. The agent receives a reward of +1 if it reaches the goal (within an L2 distance of 5) and 0 elsewhere. The Ant starts at one end of a U-shaped corridor and must navigate to the goal location at the other end. This task is particularly challenging since the reward is extremely sparse.

We again compare PGIF-versions of SAC and PPO to vanilla SAC and PPO-LSTM. Results are presented in Table 2, where we see that the baselines are unable to make any progress on this challenging task, while PGIF is able to solve the task to a point where it successfully navigates to the goal location in the maze 50% of the time. We hypothesize our algorithm has benefits in these environments since as soon as it obtains a reward signal it can adapt quickly and make use of the signal by incorporating it in both policy and value optimization, therefore accelerating learning.

Method	Mean Episodic Reward
PPO-LSTM	0.00 ± 0.00
SAC	0.00 ± 0.00
PGIF-PPO (VPN)	0.20 ± 0.13
PGIF-PPO (Force)	0.30 ± 0.15
PGIF-SAC (VPN)	0.40 ± 0.16
PGIF-SAC (Force)	0.50 ± 0.16

Table 2: Mean episodic reward on the AntMaze environment over 10 random seeds trained with 3 million environment steps. A sparse reward of +1 is obtained at the end of the episode if the agent successfully reaches the goal state within an L2 distance of 5. The number after \pm is the standard error.

5.3 Partial Observability

We now aim to show that our method is not only effective in fully-observed Markovian settings, but also in environments with partial observability. This set of experiments uses the MuJoCo robotics simulator [42] suite of continuous control tasks. These are a set of popular environments used in both online and offline deep RL works [10, 9] and provides an easily comparable benchmark for evaluating algorithm sample efficiency and reward performance. As in previous work [50], we introduce an easy modification to these tasks to make the environment partially observable thereby increasing the difficulty: We zero-out a random dimension of the state space at each data collection step. This helps us replicate a more realistic scenario for a robotic agent where not all of the state space is accessible.

We compare a PGIF-style SAC implementation to vanilla SAC and PPO-LSTM on these domains. We show the results of these experiments in Fig. 2. We find that PGIF can provide improved performance

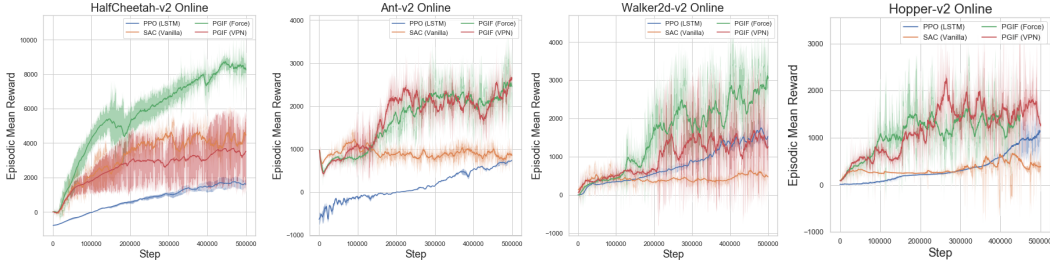


Figure 2: The online episodic mean reward evaluated over 5 episodes every 500 steps for MuJoCo continuous control RL tasks with partial observability. We show the average over 5 random seeds. 500,000 environment step interactions are used. The shaded area shows the standard error.

on these difficult tasks, suggesting that PGIF is able to leverage future information in the trajectory to appropriately avoid uncertainties about the environment, more so than when only conditioning on the immediate state (vanilla SAC) or even when conditioning on the entire past trajectory (PPO-LSTM). Interestingly, we find that the simple state based forcing (Force) performs more consistently better than the more sophisticated VPN based forcing. See the Appendix for additional results, including online evaluations without partial observability.

5.4 Offline RL Evaluations

To assess if our method is effective in an offline RL setting, we evaluate our proposed algorithm in several continuous control offline RL tasks [8] against Behavior Regularized Actor Critic (BRAC) [48] and Batch-Constrained Q-learning (BCQ) [10]. BRAC operates as a straightforward modification of SAC, penalizing the value function using a measure of divergence (KL) between the behaviour policy and the learned agent policy. For our PGIF algorithm, we use BRAC as the starting point.

For these offline MuJoCo tasks, we examine D4RL datasets classified as *medium* (where the training of the agent is ended after achieving a "medium" level performance) and *medium expert* (where medium and expert data is mixed) [8]. Datasets that contain these sub-optimal trajectories present a realistic problem for offline RL algorithms. We also include an offline version of the AntMaze, which is particularly challenging due to sparse rewards. We show the results of these experiments in Table 3. We find that our method outperforms the baselines in all but one of the tasks in terms of final episodic reward. We hypothesize in the medium-expert setting that we perform slightly worse due to the lack of action diversity which makes learning a dynamics representation difficult. Interestingly, in contrast to the online results, we find that VPN based forcing performs better than state based forcing, although even state based forcing usually performs better than the baseline methods.

Environment	BRAC	PGIF (VPN)	PGIF (Force)	BCQ
ant-medium	2731 \pm 329	3250 \pm 125	2980 \pm 164	1851 \pm 94
ant-medium-expert	2483 \pm 329	3048 \pm 362	2431 \pm 417	2010 \pm 133
hopper-medium	1757 \pm 183	2327 \pm 399	1930 \pm 44	1722 \pm 166
walker2d-medium	3687 \pm 25	3989 \pm 259	3821 \pm 341	2653 \pm 301
halfcheetah-medium	5462 \pm 198	6037 \pm 324	6231 \pm 303	4722 \pm 206
halfcheetah-medium-expert	5580 \pm 105	5418 \pm 76	5491 \pm 143	4463 \pm 88
antmaze-umaze	0.5 \pm 0.16	0.95 \pm 0.0	0.7 \pm 0.15	0.8 \pm 0.13

Table 3: Performance on the offline RL tasks showing the average episodic return. The final average return is shown after training the algorithm for 500,000 episodes and then evaluating the policy over 5 episodes. Results show an average of 5 random seeds. The value after \pm shows the standard error.

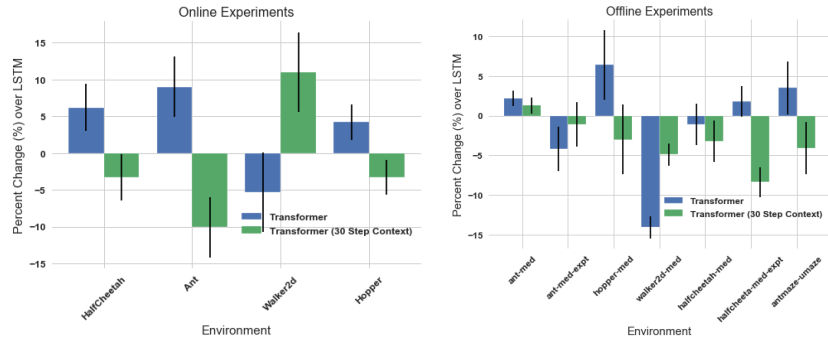


Figure 3: The percent improvement evaluated over 5 episodes by replacing the LSTM backwards network with a transformer. The 30 timestep transformer has a context size of a 30 timesteps look-ahead into the future of the trajectory. We show the average over 5 random seeds taking the final policy evaluation mean episodic reward as the value. 500,000 environment step interactions are used. The error bars shows the standard error.

5.5 Transformers Experiments

Using transformers for processing the future trajectory into latent variables offers a few key benefits over traditional RNN architectures, namely better computational efficiency with long sequences and improved ability to model long timescale interactions. These provide a few interesting benefits for use with our architecture, namely due to the fact that some of our environments generate sequences up to 1000 timesteps, which can be onerous for an RNN to process. In the following experiments, we simply replace our RNN with a transformer. This is inspired by work that models trajectories using a transformer [15] for offline RL. Additionally, we show the results of experiments where we use a K -fixed length context of future states as the input to our transformer. A short length context is much faster to process than the entire sequence of upstream states, but there is a decrease in performance, suggesting that the entire trajectory contains useful information. We show these results in Figure 3. The run-time of training was decreased by approximately 40%.

6 Discussion

In this work, we consider the problem of incorporating information from the entire trajectory in model-free online and offline RL algorithms, enabling an agent to use information about the future to accelerate and improve its learning. Our empirical results attest to the versatility of our method. The benefits of our method are apparent in both online and offline settings, which is a rare phenomenon given that many previous offline RL works suggest that what works well in online RL often transfers poorly to offline settings, and vice versa. Beyond just online and offline RL, our results encompass partial observability, sparse rewards, delayed rewards, and sub-optimal datasets, demonstrating the ability for PGIF to achieve higher reward faster in all settings.

Our work provides many interesting directions for future work. Namely, one interesting avenue would be to combine our method with exploration strategies in addition to credit assignment. Perhaps there are benefits in decreasing access to future information during initial exploratory agent steps so the agent is better able to explore. One could also incorporate a metric for surprise to *gate* access to this future information in states of high novelty.

We also wish to highlight potential risks in our work. Specifically, the use of future information in PGIF may exacerbate biases present in the experience or offline dataset. For example, it is known that expert datasets lack action diversity. Further conditioning on the future in this dataset could force these biases to be incorporated more easily into the learning algorithm.

References

- [1] Combined reinforcement learning via abstract representations. *Proceedings of the AAAI Conference on Artificial Intelligence*, 2019.

- [2] Zaheer Abbas, Samuel Sokota, Erin Talvitie, and Martha White. Selective dyna-style planning under limited model capacity. In *Proceedings of the 37th International Conference on Machine Learning*.
- [3] Justin Bayer and Christian Osendorfer. Learning stochastic recurrent networks, 2015.
- [4] Samy Bengio, Oriol Vinyals, Navdeep Jaitly, and Noam Shazeer. Scheduled sampling for sequence prediction with recurrent neural networks. In *Proceedings of the 28th International Conference on Neural Information Processing Systems*, 2015.
- [5] Jacob Buckman, Danijar Hafner, George Tucker, Eugene Brevdo, and Honglak Lee. Sample-efficient reinforcement learning with stochastic ensemble value expansion. In *Advances in Neural Information Processing Systems*, 2018.
- [6] Keith Bush and Joelle Pineau. Manifold embeddings for model-based reinforcement learning under partial observability. In *Advances in Neural Information Processing Systems*, 2009.
- [7] Carlos Florensa, David Held, Markus Wulfmeier, Michael Zhang, and Pieter Abbeel. Reverse curriculum generation for reinforcement learning. *Proceedings of Machine Learning Research*, 2017.
- [8] Justin Fu, Aviral Kumar, Ofir Nachum, George Tucker, and Sergey Levine. D4rl: Datasets for deep data-driven reinforcement learning, 2020.
- [9] Scott Fujimoto, Herke van Hoof, and David Meger. Addressing function approximation error in actor-critic methods. In *Proceedings of the 35th International Conference on Machine Learning*, 2018.
- [10] Scott Fujimoto, David Meger, and Doina Precup. Off-policy deep reinforcement learning without exploration. In *Proceedings of the 36th International Conference on Machine Learning*, 2019.
- [11] Anirudh Goyal, Alessandro Sordoni, Marc-Alexandre Côté, Nan Rosemary Ke, and Yoshua Bengio. Z-forcing: Training stochastic recurrent networks. In *Proceedings of the 31st International Conference on Neural Information Processing Systems*, 2017.
- [12] Anirudh Goyal, Alex Lamb, Jordan Hoffmann, Shagun Sodhani, Sergey Levine, Yoshua Bengio, and Bernhard Schölkopf. Recurrent independent mechanisms. In *International Conference on Learning Representations*, 2021.
- [13] Tuomas Haarnoja, Aurick Zhou, Pieter Abbeel, and Sergey Levine. Soft actor-critic: Off-policy maximum entropy deep reinforcement learning with a stochastic actor. In *Proceedings of the 35th International Conference on Machine Learning*, 2018.
- [14] Anna Harutyunyan, Will Dabney, Thomas Mesnard, Mohammad Gheshlaghi Azar, Bilal Piot, Nicolas Heess, Hado P van Hasselt, Gregory Wayne, Satinder Singh, Doina Precup, and Remi Munos. Hindsight credit assignment. In *Advances in Neural Information Processing Systems*, 2019.
- [15] Michael Janner, Qiyang Li, and Sergey Levine. Reinforcement learning as one big sequence modeling problem. *arXiv preprint arXiv:2106.02039*, 2021.
- [16] Philip N. Johnson-Laird. Mental models and human reasoning. *Proceedings of the National Academy of Sciences*, 2010.
- [17] M. Karl, Maximilian Sölch, J. Bayer, and P. V. D. Smagt. Deep variational bayes filters: Unsupervised learning of state space models from raw data. *ArXiv*, abs/1605.06432, 2017.
- [18] Nan Rosemary Ke, Amanpreet Singh, Ahmed Touati, Anirudh Goyal, Yoshua Bengio, Devi Parikh, and Dhruv Batra. Modeling the long term future in model-based reinforcement learning. In *International Conference on Learning Representations*, 2019.
- [19] Aviral Kumar, Justin Fu, Matthew Soh, George Tucker, and Sergey Levine. Stabilizing off-policy q-learning via bootstrapping error reduction. In *Advances in Neural Information Processing Systems*, 2019.
- [20] Alex M Lamb, Anirudh Goyal, Ying Zhang, Saizheng Zhang, Aaron C Courville, and Yoshua Bengio. Professor forcing: A new algorithm for training recurrent networks. In *Advances in Neural Information Processing Systems*, 2016.
- [21] Thomas Mesnard, Theophane Weber, Fabio Viola, Shantanu Thakoor, Alaa Saade, Anna Harutyunyan, Will Dabney, Thomas S Stepleton, Nicolas Heess, Arthur Guez, Eric Moulines, Marcus Hutter, Lars Buesing, and Remi Munos. Counterfactual credit assignment in model-free reinforcement learning. In *Proceedings of the 38th International Conference on Machine Learning*, 2021.

- [22] Volodymyr Mnih, Adria Puigdomenech Badia, Mehdi Mirza, Alex Graves, Timothy Lillicrap, Tim Harley, David Silver, and Koray Kavukcuoglu. Asynchronous methods for deep reinforcement learning. In *Proceedings of The 33rd International Conference on Machine Learning*.
- [23] Ofir Nachum, Bo Dai, Ilya Kostrikov, Yinlam Chow, Lihong Li, and Dale Schuurmans. Algaedice: Policy gradient from arbitrary experience, 2019.
- [24] Chris Nota, Philip Thomas, and Bruno C. Da Silva. Posterior value functions: Hindsight baselines for policy gradient methods. In *Proceedings of the 38th International Conference on Machine Learning*, 2021.
- [25] Junhyuk Oh, Satinder Singh, and Honglak Lee. Value prediction network. In *Advances in Neural Information Processing Systems*, 2017.
- [26] Ian Osband, Yotam Doron, Matteo Hessel, John Aslanides, Eren Sezener, Andre Saraiva, Katrina McKinney, Tor Lattimore, Csaba Szepesvári, Satinder Singh, Benjamin Van Roy, Richard Sutton, David Silver, and Hado van Hasselt. Behaviour suite for reinforcement learning. In *International Conference on Learning Representations*, 2020.
- [27] Georg Ostrovski, Marc G. Bellemare, Aäron van den Oord, and Rémi Munos. Count-based exploration with neural density models. In *Proceedings of the 34th International Conference on Machine Learning*, 2017.
- [28] Razvan Pascanu, Yujia Li, Oriol Vinyals, Nicolas Heess, Lars Buesing, Sebastien Racanière, David Reichert, Théophane Weber, Daan Wierstra, and Peter Battaglia. Learning model-based planning from scratch, 2017.
- [29] Deepak Pathak, Pulkit Agrawal, Alexei A. Efros, and Trevor Darrell. Curiosity-driven exploration by self-supervised prediction. In *Proceedings of the 34th International Conference on Machine Learning*, 2017.
- [30] Baolin Peng, Xiujuan Li, Jianfeng Gao, Jingjing Liu, and Kam-Fai Wong. Deep Dyna-Q: Integrating planning for task-completion dialogue policy learning. In *Proceedings of the 56th Annual Meeting of the Association for Computational Linguistics*, 2018.
- [31] Sébastien Racanière, Theophane Weber, David Reichert, Lars Buesing, Arthur Guez, Danilo Jimenez Rezende, Adria Puigdomènech Badia, Oriol Vinyals, Nicolas Heess, Yujia Li, Razvan Pascanu, Peter Battaglia, Demis Hassabis, David Silver, and Daan Wierstra. Imagination-augmented agents for deep reinforcement learning. In *Advances in Neural Information Processing Systems*, 2017.
- [32] Andrew Michael Saxe, Yamini Bansal, Joel Dapello, Madhu Advani, Artemy Kolchinsky, Brendan Daniel Tracey, and David Daniel Cox. On the information bottleneck theory of deep learning. In *International Conference on Learning Representations*, 2018.
- [33] John Schulman, Philipp Moritz, Sergey Levine, Michael Jordan, and Pieter Abbeel. High-dimensional continuous control using generalized advantage estimation. In *Proceedings of the Fourth International Conference on Learning Representations*, 2016.
- [34] John Schulman, Filip Wolski, Prafulla Dhariwal, Alec Radford, and Oleg Klimov. Proximal policy optimization algorithms. *arXiv*, 1707.06347, 2017.
- [35] Satinder P. Singh. Learning without state-estimation in partially observable markovian decision processes. In *Proceedings of the Eleventh International Conference on Machine Learning*, 1994.
- [36] Nobuo Suematsu and Akira Hayashi. A reinforcement learning algorithm in partially observable environments using short-term memory. In *Advances in Neural Information Processing Systems*, 1999.
- [37] Richard S. Sutton. Learning to predict by the methods of temporal differences. *Machine Learning*, 1988.
- [38] Richard S. Sutton. Dyna, an integrated architecture for learning, planning, and reacting. *SIGART Bull.*, 1991.
- [39] Richard S. Sutton and Andrew G. Barto. *Reinforcement Learning: An Introduction*. A Bradford Book, 2018. ISBN 0262039249.
- [40] Richard S. Sutton, David McAllester, Satinder Singh, and Yishay Mansour. Policy gradient methods for reinforcement learning with function approximation. In *Proceedings of the 12th International Conference on Neural Information Processing Systems*, 1999.
- [41] Naftali Tishby, Fernando C. Pereira, and William Bialek. The information bottleneck method. 1999.

- [42] E. Todorov, T. Erez, and Y. Tassa. MuJoCo: A physics engine for model-based control. In *2012 IEEE/RSJ International Conference on Intelligent Robots and Systems*, 2012.
- [43] John N. Tsitsiklis and Benjamin Van Roy. Analysis of temporal-difference learning with function approximation. In *Proceedings of the 9th International Conference on Neural Information Processing Systems*, 1996.
- [44] Hado van Hasselt, Yotam Doron, Florian Strub, Matteo Hessel, Nicolas Sonnerat, and Joseph Modayil. Deep reinforcement learning and the deadly triad, 2018.
- [45] Ashish Vaswani, Noam Shazeer, Niki Parmar, Jakob Uszkoreit, Llion Jones, Aidan N Gomez, Łukasz Kaiser, and Illia Polosukhin. Attention is all you need. In *Advances in neural information processing systems*, pages 5998–6008, 2017.
- [46] Tingwu Wang, Xuchan Bao, Ignasi Clavera, Jerrick Hoang, Yeming Wen, Eric Langlois, Shunshi Zhang, Guodong Zhang, Pieter Abbeel, and Jimmy Ba. Benchmarking model-based reinforcement learning, 2020.
- [47] Lex Weaver and Nigel Tao. The optimal reward baseline for gradient-based reinforcement learning. In *Proceedings of the Seventeenth Conference on Uncertainty in Artificial Intelligence*, 2001.
- [48] Yifan Wu, George Tucker, and Ofir Nachum. Behavior regularized offline reinforcement learning, 2020. URL <https://openreview.net/forum?id=BJg9hTNKPH>.
- [49] Markus Wulfmeier, Dushyant Rao, Roland Hafner, Thomas Lampe, Abbas Abdolmaleki, Tim Hertweck, Michael Neunert, Dhruva Tirumala, Noah Siegel, Nicolas Heess, and Martin Riedmiller. Data-efficient hindsight off-policy option learning, 2021.
- [50] Mengjiao Yang and Ofir Nachum. Representation matters: Offline pretraining for sequential decision making, 2021.
- [51] Chi Zhang, Sanmukh Rao Kuppannagari, and Viktor Prasanna. {BRAC}+: Going deeper with behavior regularized offline reinforcement learning, 2021. URL <https://openreview.net/forum?id=bMCfFepJXM>.
- [52] Łukasz Kaiser, Mohammad Babaeizadeh, Piotr Miłoś, Błażej Osipiński, Roy H Campbell, Konrad Czechowski, Dumitru Erhan, Chelsea Finn, Piotr Kozakowski, Sergey Levine, Afroz Mohiuddin, Ryan Sepassi, George Tucker, and Henryk Michalewski. Model based reinforcement learning for atari. In *International Conference on Learning Representations*, 2020.

A Implementation Considerations

We will introduce some implementation details for our model, specifically how the parameters for each distribution are learned.

Data Collection Model: In the first phase of the actor critic process we are in a *generation* phase of the data. Here, we have a prior over the latent variables $p_{vz}(z_t)$. This prior distribution can be defined as a Gaussian distribution with parameters as $p_{vz}(z_t) = \mathcal{N}(z_t; \mu_t^Z, \log \sigma_t^Z)$. To learn the parameters of this Gaussian prior we utilize an MLP (f) defined by $[\mu_t^Z, \log \sigma_t^Z] = f^Z(s_t)$ which takes the current state as input.

Now that we have the learned parameters, we can sample $z_t \sim p_{vz}(z_t)$ using the reparameterization trick given the learned mean and standard deviation. We denote this as $z_t \sim \text{reparameterize}(\mu_t^Z, \log \sigma_t^Z)$. At each time-step during the generation phase, we encounter a state from our environment. We find the distribution parameters and then sample z_t as denoted previously. The latent variable policy is then executed: $a_t \sim \pi_\theta(a_t|s_t, z_t)$. By applying action a_t on the environment we then obtain s_{t+1}, r_t , and repeat until termination. This leaves us with a sequence of states for use in inference. We denote the full trajectories generated in this phase with, τ , and $\tau_{(s)} = \{s_0, \dots, s_T\}$ being the trajectories only containing states. Let us define the set of state only trajectories as, $\{\tau_{(s)}^0, \dots, \tau_{(s)}^n\} \in \mathcal{D}_{(s)}$.

Training Model: The 2nd part of our actor critic algorithm where we learn the policy using the data in the inference phase. This is where we approximate the true posterior distribution over our latent variables. As in Z-forcing, we will use a *backwards* RNN, which takes the reversed sequence of states, $\tau_{(s)}^\leftarrow$ as input. We define this network as,

$$b_t = f^\leftarrow(s_{t+1}, b_{t+1}). \quad (11)$$

Each state b_t therefore contains information about future states and can be used to shape the approximate posterior distribution over latent variables to contain this information. We define the inference network with a normal distribution,

$$q_{\phi^Z}(z_t|b_t) = \mathcal{N}(z_t; \mu_t^q, \log \sigma_t^q), \quad (12)$$

where, as before, the parameters are learned with an MLP defined by $[\mu_t^q, \log \sigma_t^q] = f^q(b_t)$.

We derive a conditional generative model $p_\zeta(b|z)$ over the backwards states given the inferred latent variables $z_t \sim q_{\phi^Z}(z_t|b_t)$. Similar to before, we define the parameters of this Gaussian as $p_\zeta(b_t|z_t) = \mathcal{N}(z_t; \mu_t^{\text{Ax}}, \log \sigma_t^{\text{Ax}})$, with a MLP that produces $[\mu_t^{\text{Ax}}, \log \sigma_t^{\text{Ax}}] = f^{\text{Ax}}(z_t)$.

B Full Algorithm

We show the full algorithms for PGIF-PPO (Algorithm 2) with State based forcing and PGIF-SAC (Algorithm 4) with state based forcing in this section. Using VPN forcing simply changes the auxiliary loss calculations. The shared Backwards RNN Pass algorithm is in Algorithm 3.

Algorithm 2 Algorithm with Advantage Policy Gradient and State Based Forcing

Require: Initial policy parameters: θ , Prior parameters: v^Z, ϕ^Z , KL weight: β , Auxiliary loss Parameters: θ^{Ax} , Auxiliary loss weight: α Backwards net input parameters: θ^{in} , Backwards RNN parameters: θ^{bkw} , Backwards net output parameters: $\theta^{\text{bkw-out}}$, Initial hidden states \mathbf{h}_i .

- 1: **for** policy-step $k = 0, 1, 2, \dots, N$ **do**
- 2: Collect set of Trajectories $\mathcal{D} = \{\tau_i, \dots\}$:
- 3: **repeat**
- 4: $[\mu_t^Z, \log \sigma_t^Z] = f_{v^Z}(s_t)$
- 5: $z_t \sim \text{reparameterization}(\mu_t^Z, \log \sigma_t^Z)$
- 6: Execute: $\pi_\theta(a_t|s_t, z_t) = f_\theta(s_t, z_t)$
- 7: Observe s_{t+1}, r_t from environment.
- 8: $\tau_i = \tau_i \cup \{s_t, a_t, s_{t+1}, r_t\}$
- 9: **until** episode termination
- 10: Compute advantage estimates \hat{A}_t^k using GAE.
- 11: **for** Trajectory: $\tau_i \in \mathcal{D}$ **do**
- 12: $\mathbf{b}_i, \mathbf{h}_i = \text{BackwardsPass}(\tau_i, \mathbf{h}_i, \theta^{(\text{in})}, \theta^{\text{bkw}}, \theta^{\text{bkw-out}})$
- 13: $\tau_i = \tau_i \cup \{\mathbf{b}_i\}$
- 14: Reset: $J_{\text{PG}} = 0$
- 15: **for** timestep $t \in \{0, \dots, T\}$ **do**
- 16: $\forall \{s_t, b_t, a_t\} \in \mathcal{D}: [\mu_t^Z, \log \sigma_t^{\text{Z-PG}}] = f_{\phi^Z}(b_t, s_t)$
- 17: $z_t^{\text{PG}} \sim \text{reparameterization}(\mu_t^{\text{Z-PG}}, \log \sigma_t^{\text{Z-PG}})$
- 18: $\pi_\theta(a_t|s_t, z_t^{\text{PG}}) = f_\theta(s_t, z_t^{\text{PG}})$
- 19: $[\mu_t^{\text{Ax}}, \log \sigma_t^{\text{Ax}}] = f_{\theta^{\text{Ax}}}(z_t^{\text{PG}})$
- 20: $J_{\text{KL}} = \text{KLDivergence}(\mu_t^{\text{Z-PG}}, \log \sigma_t^{\text{Z-PG}}, \mu_t^Z, \log \sigma_t^Z)$
- 21: $J_{\text{Ax}} = \text{LogProbGaussian}(b_t, \mu_t^{\text{Ax}}, \log \sigma_t^{\text{Ax}})$
- 22: $J_{\text{PG}} \stackrel{+}{=} \mathbb{E}_{\tau_i \in \mathcal{D}} \left[\log \pi_\theta(a_t|s_t, z_t^{\text{PG}}) \hat{A}_t^k \right] - \alpha J_{\text{Ax}} - \beta J_{\text{KL}}$
- 23: Update all parameters w.r.t: J_{PG}
- 24: Update value function estimates with any method.

Algorithm 3 BackwardsPass

Require: Trajectory: τ , Hidden states h , Input MLP Parameters: θ^{in} , Backwards RNN Parameters: θ^{bkw} , Output net parameters: $\theta^{\text{bkw-out}}$.

- 1: $\tau^{-1} = \text{Reverse-Order}(\tau)$
- 2: $x_{\text{bkw}} = f_{\theta^{\text{in}}}(\tau^{-1})$
- 3: $h_{\text{bkw}} = f_{\theta^{\text{bkw}}}(x_{\text{bkw}}, h)$ (Operates over the entire sequence)
- 4: $x_{\text{bkw-out}} = f_{\theta^{\text{bkw-out}}}(h_{\text{bkw}})$
- 5: $x_{\text{bkw-out}} = \text{Reverse-Order}(x_{\text{bkw-out}})$
- 6: $h_{\text{bkw}} = \text{Reverse-Order}(h_{\text{bkw}})$
- 7: **return** $x_{\text{bkw-out}}, h_{\text{bkw}}$

C Experimental Parameters

In this section, we give the hyperparameters used for each of our experiments in Tables 4, 5, and 6.

Algorithm 4 SAC Algorithm with State Based Forcing

Require: Initial policy parameters: θ , Z forcing parameters: v^Z, v^U, ϕ^Z, ϕ^U , KL weight: β , Auxiliary loss Parameters: $\theta^{\text{Ax-PG}}, \theta^{\text{Ax-TD}}$, Auxiliary loss weight: α Backwards net input parameters: $\theta^{\text{in}}, \theta^{\text{in-Z}}, \theta^{\text{in-U}}, \theta^{\text{in-TD}}$, Backwards RNN parameters: $\theta^{\text{bkw-Z}}, \theta^{\text{bkw-U}}, \theta^{\text{bkw-out-Z}}, \theta^{\text{bkw-out-U}}$, Backwards net output parameters: $\theta^{\text{bkw-out-Z}}, \theta^{\text{bkw-out-U}}$, Initial hidden states $\mathbf{h}_i^Z, \mathbf{h}_i^U$.

```

1: for policy-step  $k = 0, 1, 2, \dots, N$  do
2:   Collect set of Trajectories  $\mathcal{D} = \{\tau_i, \dots\}$  :
3:   repeat
4:      $[\mu_t^Z, \log \sigma_t^Z] = f_{v^Z}(s_t)$ 
5:      $z_t \sim \text{reparameterization}(\mu_t^Z, \log \sigma_t^Z)$ 
6:     Execute:  $\pi_\theta(a_t|s_t, z_t) = f_\theta(s_t, z_t)$ 
7:     Observe  $s_{t+1}, r_t$  from environment.
8:      $\tau_i = \tau_i \cup \{s_t, a_t, s_{t+1}, r_t\}$ 
9:   until episode termination
10:  for Trajectory:  $\tau_i \in \mathcal{D}$  do
11:     $\mathbf{b}_i^Z, \mathbf{h}_i^Z = \text{BackwardsPass}^Z(\tau_i, \mathbf{h}_i^Z, \theta^{\text{in-Z}}, \theta^{\text{bkw-Z}}, \theta^{\text{bkw-out-Z}})$ 
12:     $\mathbf{b}_i^U, \mathbf{h}_i^U = \text{BackwardsPass}^U(\tau_i, \mathbf{h}_i^U, \theta^{\text{in-U}}, \theta^{\text{bkw-U}}, \theta^{\text{bkw-out-U}})$ 
13:     $\tau_i = \tau_i \cup \{\mathbf{b}_i^U, \mathbf{b}_i^Z\}$ 
14:  Reset:  $J_{\text{PG}}, J_Q = 0$ 
15:  for timestep  $t \in \{0, \dots, T\}$  do
16:     $\forall \{s_t, b_t, a_t, s_{t+1}, b_t^Z, b_t^U\} \in \mathcal{D}$ 
17:    Compute  $a_{t+1}$ 
18:     $[\mu_{t+1}^Z, \log \sigma_{t+1}^Z] = f_{v^Z}(s_{t+1})$ 
19:     $z_{t+1} \sim \text{reparameterization}(\mu_{t+1}^Z, \log \sigma_{t+1}^Z)$ 
20:     $a_{t+1} \sim \pi_\theta(a_{t+1}|s_{t+1}, z_{t+1}) = f_\theta(s_{t+1}, z_{t+1})$ 
21:    Compute target Q (U-Tar to denote distribution parameters)
22:     $[\mu_{t+1}^{\text{U-Tar}}, \log \sigma_{t+1}^{\text{U-Tar}}] = f_{v^U}(s_{t+1})$ 
23:     $u_{t+1}^{\text{Tar}} \sim \text{reparameterization}(\mu_{t+1}^{\text{U-Tar}}, \log \sigma_{t+1}^{\text{U-Tar}})$ 
24:     $y(r_t, s_{t+1}, d) = r_t + \gamma(1 - d) \left( Q_{\psi\text{-target}}(s_{t+1}, a_{t+1}, u_{t+1}^{\text{Tar}}) - \alpha \log \pi_\theta(a_{t+1}|s_{t+1}, z_{t+1}) \right)$ 
25:    Update Q functions
26:     $[\mu_t^U, \log \sigma_t^U] = f_{\phi^U}(b_t^Q, s_t)$ 
27:     $u_t \sim \text{reparameterization}(\mu_t^U, \log \sigma_t^U)$ 
28:     $J_{\text{KL-TD}} = \text{KLDivergence}(\mu_t^U, \log \sigma_t^U, \mu_t^{\text{U-Tar}}, \log \sigma_t^{\text{U-Tar}})$ 
29:     $[\mu_t^{\text{Ax-TD}}, \log \sigma_t^{\text{Ax-TD}}] = f_{\theta^{\text{Ax-TD}}}(u_t)$ 
30:     $J_{\text{Ax-TD}} = \text{LogProbGaussian}(b_t^Q, \mu_t^{\text{Ax-TD}}, \log \sigma_t^{\text{Ax-TD}})$ 
31:     $J_Q \stackrel{\pm}{=} (Q_\psi(s_t, a_t, u_t) - y(r_t, s_{t+1}, d)) + \alpha J_{\text{Ax-TD}} + \beta J_{\text{KL-TD}}$ 
32:    Update Target Networks
33:     $(\psi - \text{target}) \leftarrow \rho(\psi - \text{target}) + (1 - \rho)\psi$ 
34:    Update Policy
35:     $[\mu_t^{\text{Z-PG}}, \log \sigma_t^{\text{Z-PG}}] = f_{\phi^Z}(b_t^Z, s_t)$ 
36:     $z_t^{\text{PG}} \sim \text{reparameterization}(\mu_t^{\text{Z-PG}}, \log \sigma_t^{\text{Z-PG}})$ 
37:     $a_t \sim \pi_\theta(a_t|s_t, z_t^{\text{PG}}) = f_\theta(s_t, z_t^{\text{PG}})$ 
38:     $[\mu_t^{\text{Ax-PG}}, \log \sigma_t^{\text{Ax-PG}}] = f_{\theta^{\text{Ax-PG}}}(z_t^{\text{PG}})$ 
39:     $J_{\text{KL-PG}} = \text{KLDivergence}(\mu_t^{\text{Z-PG}}, \log \sigma_t^{\text{Z-PG}}, \mu_t^Z, \log \sigma_t^Z)$ 
40:     $J_{\text{Ax-PG}} = \text{LogProbGaussian}(b_t^Z, \mu_t^{\text{Ax-PG}}, \log \sigma_t^{\text{Ax-PG}})$ 
41:     $J_{\text{PG}} \stackrel{\pm}{=} \mathbb{E}_{\tau_i \in \mathcal{D}} \left[ Q_\psi(s_t, a_t, u_t) - \alpha \log \pi_\theta(a_t|s_t, z_t^{\text{PG}}) \right] + \alpha J_{\text{Ax-PG}} + \beta J_{\text{KL-PG}}$ 
42:  Update all parameters w.r.t:  $J_{\text{PG}}$  or  $J_Q$ 
43:  Update value function estimates with any method.

```

Parameter	Value
Optimizer	Adam
Learning rate	$5e^{-4}$
Batch size	250
Actor and Critic network dimensions	(300, 200)
RNN Dim	15
RNN-Embedding Dim	20
Z or Q Dim	5
Z-force Neural net dim	20
Initial random exploration steps	10000
Replay Buffer Size	1,000,000 steps
Discount	0.99
Evaluation Episodes	5

Table 4: Parameters used for PGIF and SAC in the online experiments with MuJoCo.

Parameter	Value
Optimizer	Adam
Learning rate	$1e^{-3}$
Value penalty	True
Batch size	250
Actor and Critic network dimensions	(300, 200)
Q value ensemble	2
RNN Dim	15
RNN-Embedding Dim	20
Z or Q Dim	10
Z-force Neural net dim	20
Initial random exploration steps	10000
Replay Buffer Size	1,000,000 steps
Discount	0.99
Evaluation Episodes	5
BRAC Value Penalty α	0.1

Table 5: Parameters used for transformers experiments

Parameter	Value
Hidden Dim	128
Activation	ReLu
Heads	1
Heads	1
Layers	3
Attention Dropout	0.1

Table 6: Parameters used for the transformers experiments.

Training the behavior policy for BRAC offline RL experiments uses behavior cloning with 300,000 time steps.

For the purpose of the backwards RNN, since we have variable episode length we pad the episode sequence to the maximum length with zeros. The maximum number of timesteps is generally 1000 in MuJoCo. The training of the RNN with this long sequence and the pre-processing steps involved are expensive computationally. For offline experiments, our replay buffer is episodic, so we train with an entire episode at each update. For online we train with a batch of randomly sampled steps from

the replay buffer (and obtain the respective episodes that those steps were in for the training of the backwards RNN).

D Online Experiment Learning Curves

In this section, we show the training curves for the online experiments with full observability in Figure 4. We compare PGIF against SAC only, since we see that PPO performs much worse from initial experiments. Note that in practicality, it is best to reduce the maximum number of steps in the MuJoCo environments to 500 for better computational efficiency in the backwards RNN steps (without much change in final reward). We note that our method appears to have a small reduction in standard error compared to vanilla SAC.

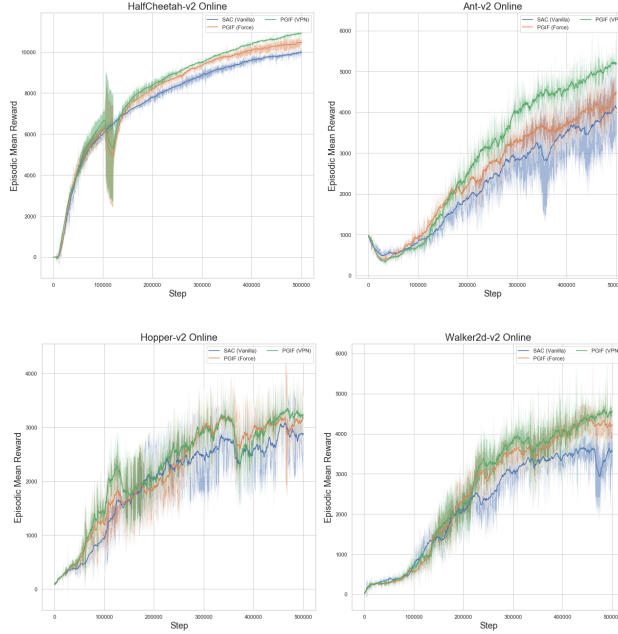


Figure 4: The online episodic mean reward evaluated over 5 episodes every 500 steps for MuJoCo continuous control RL tasks with full observability. We show the average over 5 random seeds. 500,000 environment step interactions are used. The shaded area shows the standard error.

We aim to investigate the effect PGIF learning with a lower batch size. We notice that PGIF has better performance at lower batch sizes. It may be an interesting direction to further investigate this anomaly. In Figure 5, we show the performance of PGIF with a batch size of 25.

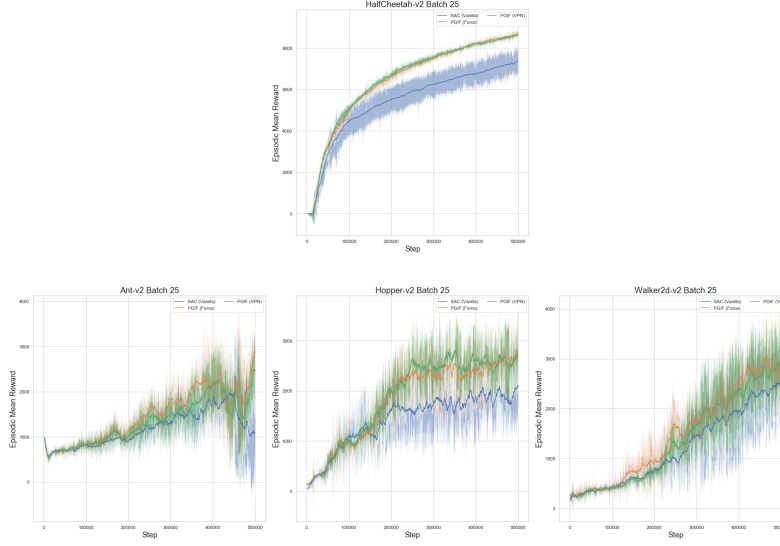


Figure 5: The online episodic mean reward evaluated over 5 episodes every 500 steps for MuJoCo tasks with full observability. We show the average over 5 random seeds. 500,000 environment step interactions are used. The model is updated with a batch size of 25. The shaded area shows the standard error.

E Computing Infrastructure

The cluster used to run these experiments has 688 NVIDIA V100-SXM2 GPUs.